Nanoscale

Accepted Manuscript

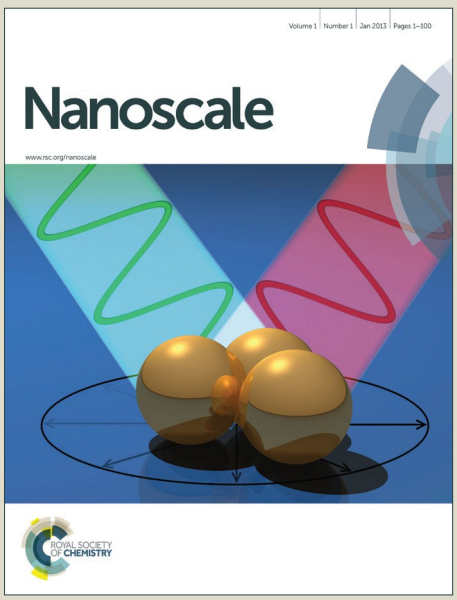

ROYAL SOCIETY OF CHEMISTRY

www.rsc.org/nanoscale

Journal Name

RSCPublishing

ARTICLE

Cite this: DOI: 10.1039/x0xx00000x

Characterization of the Bionano Interface and Mapping Extrinsic Interactions of the Corona of Nanomaterials

D.J. O'Connell,[a,b] F. Baldelli Bombelli,[e] A. S. Pitek,[a,d,f] M. P. Monopoli,[a,d] D. J. Cahill,[a,c] K. A. Dawson[a,d]

Received 00th January 2012,
Accepted 00th January 2012

DOI: 10.1039/x0xx00000x

www.rsc.org/

[a] Conway Institute for Biomolecular and Biomedical Research, University College Dublin, Ireland, [b] School of Biomolecular & Biomedical Science, University College Dublin, Dublin, Ireland, [c] School of Medicine, University College Dublin, Dublin, Ireland, [d] Centre for BioNano Interactions, School of Chemistry and Chemical Biology, University College Dublin, Dublin, Ireland; [e] Current address: Department of Chemistry, Materials and Chemical Engineering, Politecnico di Milano, Milano, Italy; [f] Department of Biomedical Engineering, School of Medicine, Case Western Reserve University, Cleveland OH, USA.

kenneth.a.dawson@cbni.ucd.ie
DO'C & FBB contributed equally

Nanoparticles in physiological environments are known to selectively adsorb proteins and other biomolecules forming a tightly bound biomolecular 'corona' on their surface. Where the exchange times of the proteins are sufficiently long, it is believed that the protein corona constitutes the particle identity in biological milieu. Here we show that proteins in the corona retain their functional characteristics and can specifically bind to cognate proteins on arrays of thousands of immobilised human proteins. The biological identity of the nanomaterial is seen to be specific to the blood plasma concentration in which they are exposed. We show that the resulting *in situ* nanoparticle interactome is dependent on the protein concentration in plasma, with the emergence of a small number of dominant protein-protein interactions. These interactions are those driven by proteins that are adsorbed onto the particle surface and whose binding epitopes are subsequently expressed or presented suitably on the particle surface. We suggest that, since specific tailored protein arrays for target systems and organs can be designed, their use may be an important element in an overall study of the biomolecular corona.

Introduction

Identifying 'what the cell sees' in a physiological environment, rather than the pristine nanoparticle surface, would give new insight and clarity to the development of nanomedicine and nanosafety. [1-4] Whatever the nature of the original nanoparticle surface, its modification by selective adsorption of biomolecules (such as proteins, lipids and glycans)[5] from the surrounding biological milieu, can lead to a long-lived biomolecular identity that has been termed the 'hard' protein corona.[5-13] A typical hard corona lifetime for a common engineered nanomaterial can be of many hours, which is likely to be sufficiently long for the surface of the corona to constitute the primary functional interface between nanomaterials and the biological processing machinery.[4] Even where slow replacement of one set of biomolecules by another does take place *in situ*, the slowly exchanging component of the new corona is likely to be the biologically relevant aspect that defines the system, while the bare surface remains buried.[6, 14-20] Although the corona composition can now be systematically determined, we expect the exposed outer surface (*de facto* the bionano interface) to be the biologically relevant aspect in recognition by biological systems. Early studies have already highlighted that the corona exposes specific epitopes

that are specific to the nanoparticle surface propriety, [21, 22] and to the time and the biological media in which they are exposed.[5 11, 23, 24]
In this paper we report the striking outcome that the suppression of the nanoparticle identity by the corona in a biological environment results in a small number of well-defined biological interactions providing an emergent context-dependent biological identity.
Evidently the relationships between the nanomaterial surface, its adsorbed biomolecules and the potential biomolecular binding sites projecting from the surface of the hard corona (across the hard-soft corona interface) may not be simple.[14, 25-28] For example, biomolecular packing in the corona, the protein conformational disruptions, and the unusual juxtaposition of proteins on the nanoparticle surface all affect the final epitopes displayed by the nanoparticle-hard corona complex. Here we determine the interactions of several model nanoparticles incubated, in the presence of human plasma, with 9,483 full-length, purified human proteins expressed in a eukaryotic expression system on high content human protein microarrays. In biological systems, not all of these proteins will be accessible to plasma-borne particles, but the resulting interaction pattern ('interactome') usefully represents the *in situ* biological identity of the particles in the plasma concentration chosen. In this work we link the nature of the adsorbed protein (as derived from proteomics and other techniques) to the protein binding targets, potentially providing a mechanistic link between what is adsorbed and what is targeted. We find that, unsurprisingly (due to their high surface energy), in the absence of plasma all studied nanoparticles bind non-specifically to most proteins on the array to different degrees. However, in the presence of increasing human plasma concentration, the hard corona forms and the non-specific interactions of nanoparticles with all of the arrayed proteins progressively diminishes as the bare nanoparticle surface is covered. At yet higher plasma concentrations, specific interactions between the corona and target proteins emerge. Conversely, the interactions with array proteins for which there are no specific interactions continue to decrease. It is clear from our studies that nanoparticle incubation in plasma, over a time course, results in strikingly similar protein corona composition patterns and results in a conserved interactome with microarray proteins. This is seen along with small changes in protein corona composition and is accompanied by a gradual increase in protein corona shell thickness (extrapolated from DCS data) reaching a "plateau" state with time. For longer exposure times, as the protein corona equilibrates, a monotonic increase in total intensity of binding spots occurs up to four hours of incubation time.

Results

Physical Characterization of Polystyrene Nanoparticles. Carboxylated polystyrene nanoparticles, PSCOOH, of different sizes (nominally 40 nm and 100 nm) and sulphonated polystyrene nanoparticles, $PSOSO_3$, (nominally 100 nm) were incubated either in physiological buffer or in human plasma and have been characterized by dynamic light scattering (DLS), Z-potential, differential centrifugal sedimentation (DCS), 1D gel electrophoresis (Figure 1, figure S1 and Table S1). Nanoparticle-protein complexes have been studied both *in situ* in human plasma and once removed from the biological milieu and washed (hard corona); *in situ* samples were measured in the same standardised experimental conditions as used for subsequent protein microarray experiments. All the nanoparticles in physiological buffer had a negative Z-potential (Table S1) and DLS results for PSCOOH nanoparticles showed the formation of monodispersed protein corona complexes with a significant increase of the Z-potential suggesting that the protein coating itself is the main source of the particle stability in plasma (Table S1). The more resolved differential centrifugation sedimentation (DCS) measurements confirmed that the size distribution for 40 nm PSCOOH nanoparticles was dominated by monomer protein-nanoparticle complexes with a larger apparent diameter than those of bare nanoparticles and revealed the increasing thickness of the corona, moving from PBS to 75% (v/v) human plasma in PBS (Figure 1a). A more accurate analysis of DCS results, (details of the method in Reference 3), estimated the protein shell thickness to be between 5.5 – 10 nm for 40 nm PSCOOH in plasma concentrations ranging from 1-75% (v/v) in PBS (Inset in Figure 1) and about 8.4 nm for 100 nm PSCOOH in 10% (v/v) plasma in PBS (Figure S1b). The size distribution for 100 nm sulphonated nanoparticles in physiological buffer was more polydisperse with the presence of dimers and trimers which justify the higher hydrodynamic radii and polydispersity found for this sample (Figure S1a and Table S1). Moreover, both DLS and DCS data showed that 100 nm sulphonated nanoparticles formed large aggregates in human plasma, which are most likely nanoparticle-embedded plasma aggregates (Figure S1c).

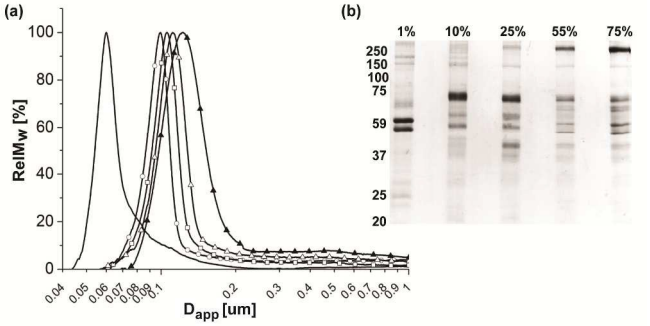

% Plasma	0	1	10	25	55	75
Apparent Diameter (nm)	60	99.3	105.5	111.2	122.6	125.7
Shell thickness (nm)	0	~5.5	~6.5	~7.5	~10	~10.5

Figure 1. DCS and 1D PAGE results of 40 nm PSCOOH nanoparticles in phosphate buffer and after 1 hour incubation in plasma concentration gradient. (A) DCS measurements of 40 nm PSCOOH nanoparticles from PBS ( ) to increasing plasma concentrations 1% (○), 10% (□), 25% (△), 55% (▲). The increase in the apparent diameter D_{app} with plasma concentration indicates an increase in the protein corona thickness. (B) Coomassie stain of PSCOOH 40 nm nanoparticle hard corona proteins from nanoparticles complexes at different human plasma concentrations 1%-75% (v/v).

Composition of the nanoparticle hard protein corona. 40 and 100 nm PSCOOH and 100 nm $PSOSO_3$ nanoparticles were incubated in human plasma at the same surface area/total protein ratio as was used in the experiments with the human protein microarrays. Strongly bound hard corona proteins were identified by mass spectrometry and the results are reported in Table 1 and Tables S2-S7. Interestingly the hard corona compositions for nanoparticles of the same surface chemistry and different size, as well were all unique. For 100 nm PSCOOH, the dominant protein identified was vitronectin, while for the 100 nm $PSOSO_3$ particles the fibrinogen beta, alpha and gamma chains predominated (Tables S6-S7).[24] For the 40 nm PSCOOH nanoparticles in increasing plasma concentrations 10-75% (v/v) in PBS, there were significant changes in the relative composition of the hard corona (Table 1). For example, there was a 10-fold decrease in the abundance of human serum albumin as the plasma concentration increased. Other

examples include a 3-fold and 4-fold increase in apolipoprotein B-100 and IgM respectively, as the plasma concentration increased. While apolipoprotein(a) was not detected in the hard corona at 10% (v/v) plasma but increased to 2.5% of the hard corona composition at 75% (v/v) plasma concentration. In addition, we measured a significant increase in fibronectin content from 0.2% to 2.9% from 10-75% (v/v) plasma concentration.

Table 1. MS results for the most abundant proteins in the hard corona of 40 nm PSCOOH nanoparticles incubated in a concentration series of human plasma. The full list of proteins in the spectrogram are listed in tables S2-S5

Acc. No[a]	Protein Identity	N% Area[b] 75%[c]	N% Area[b] 55%[c]	N% Area[b] 25%[c]	N% Area[b] 10%[c]
P04196	histidine rich glycoprotein	34.0	42.4	52.9	35.5
P04114	apolipoprotein B-100	16.1	11.9	1.8	5.1
P01871	Ig Mu heavy chain	12.0	9.6	4.7	2.9
P01042	kininogen 1	9.2	8.2	11.0	15.4
P02751	fibronectin	2.9	2.3	0.5	0.2
P03951	coagulation factor XI	2.7	1.5	1.5	1.5
P08519	apolipoprotein (a)	2.5	1.7	1.3	0.0
P04004	vitronectin	1.8	1.0	1.8	3.4
P02649	apolipoprotein E	1.5	1.6	1.7	2.6
P62736	actin, aortic smooth	1.1	0.6	0.4	0.2
P00747	plasminogen	1.1	0.6	1.1	1.1
P0C0L4	complement C4-A	1.0	0.6	0.4	0.9
P02671	fibrinogen alpha chain	0.9	0.4	0.5	0.9
P02679	fibrinogen gamma chain	0.8	0.4	0.5	0.8
P02675	fibrinogen beta chain	0.8	0.1	0.4	0.8
P01876	Ig alpha-1 chain C region	0.8	0.01	0.4	0.2
P01024	Complement C3	0.8	0.4	0.3	1.3
P01834	Ig kappa chain C region	0.8	0.5	0.2	0.4
P02768	serum albumin	0.6	0.7	0.5	6.1
P08514	Integrin alpha II-b	0.6	0.1	0.1	0.1

a. Uniprot accession number
b. Representative % area under peptide peak normalised for total area of mass spectrogram
c. Human plasma concentration (v/v)

Corona Interactome Identification The nanoparticle-corona interactome profiling on protein microarrays, was seen to be particle specific. In particular when nanoparticles were exposed to 10% (v/v) plasma prior exposure to the array, it was clear from comparison of the the protein binding patterns of 100 nm PSCOOH and 100 nm $PSOSO_3$ nanoparticles that the interactome in 10% (v/v) plasma was very distinct from that obtained for plasma free conditions. Distinct interactomes were also identified for the PSCOOH and $PSOSO_3$ surface chemistries at the same plasma concentration (Figure S2 tables S8-S12). For the 40 nm PSCOOH nanoparticle samples dispersed in PBS, we used the equivalent nanoparticle concentration (16 μg/ml), in terms of total surface area/protein ratio, to the highest concentration investigated for the 100nm PSCOOH (40 μg/ml). In plasma free conditions, there was a significant overlap (>90%) between the interactomes for 100nm PSCOOH, 40nm PSCOOH and 100nm $PSOSO_3$ nanoparticles (Figure S2).

In contrast, distinct patterns of binding for the three nanoparticle types were seen in 10% (v/v) plasma and specifically looking at the 50 highest fluorescence signals on each microarray, we saw a very low level of overlap between the arrayed proteins identified from the different nanoparticle types (Figure S3a and tables S8-S11). For 40 nm PSCOOH nanoparticles, we saw an increasing overlap of proteins in the top 50 signals at 55 & 75% plasma (Figure S3b) and with increasing plasma concentrations (10%-75% v/v), there was a significant increase in the fluorescence signal for a number of spots on the protein microarray after the initial decrease in signal intensity from PBS to 10% (v/v) plasma (see Table 2, Figure S4 and tables S12-S15).

Table 2. Fluorescence intensities of selected 40 nm PSCOOH hard corona interacting proteins.

Acc.no[a]	Protein identity	I_F[b] 75%[c]	I_F[b] 55%[c]	I_F[b] 10%[c]	I_F[b] 0%[c]
Q9Y2H6	Fibronectin type-III domain-containing protein 3A	662	277	98	626
P45984	Mitogen-activated protein kinase 9	850	855	30	84
P18031	Tyrosine-protein phosphatase non-receptor type 1	639	452	0	177
Q8IYD1	Eukaryotic peptide chain release factor GTP-binding subunit	424	44.5	341	151
Q96K21	Zinc finger FYVE domain-containing protein 19	405	0	0	197
Q13492	Phosphatidylinositol-binding clathrin assembly protein	332	0	0	217
Q9UKE5	TRAF2 and NCK-interacting protein kinase	211	32	44	0

a. Uniprot accession number
b. Fluorescence signal values related to that specific arrayed protein.
c. Human plasma concentration (v/v)

Figure S4 highlights emergent binding profile observed for fibronectin domain containing 3 A (FNDC3A), protein tyrosine phosphatase, non-receptor type 1 (PTPN1) and phosphatidylinositol binding clathrin assembly protein (PICALM). We have further characterized the binding of the nanoparticle hard corona to FNDC3A with respect to a native ligand for this receptor protein, fibronectin, which is found in increasing amounts in the composition of the hard corona from 1-75% (v/v) plasma (Figure 2 and Table 1). Using the STRING algorithm (http://string-db.org/), we illustrated the known functional interaction between FNDC3A and fibronectin that together may have an important role in regulating cell adhesion, migration and proliferation.[29, 30] We demonstrated with an anti-fibronectin antibody the increasing content of fibronectin in the 40nm PSCOOH hard corona from 10-75% (v/v) plasma and strikingly the absence of fibronectin immunoreactivity in the hard corona of 100 nm PSCOOH and 100 nm $PSOSO_3$ polystyrene at concentrations of plasma to 55% (v/v) (Figure S5).

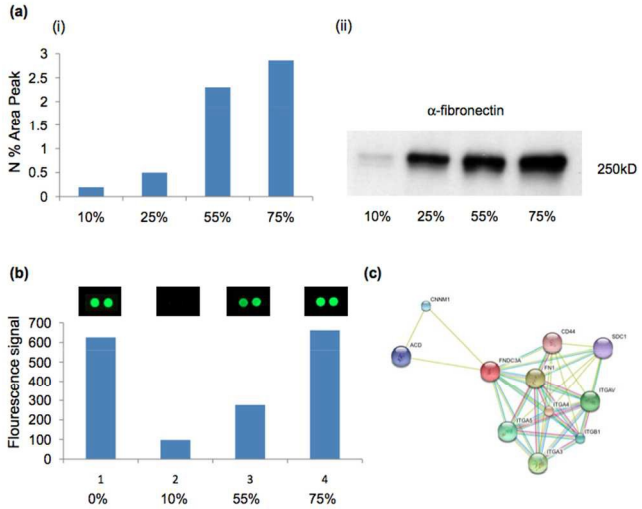

Figure 2. Interaction of hard corona protein fibronectin with arrayed fibronectin-domain containing III a (FNDC3A). (A) (i) MS spectrum fibronectin content in 40 nm PSCOOH nanoparticle hard coronas with increasing plasma concentration (x-axis) and (ii) western blot of fibronectin in the hard corona of 40 nm PSCOOH nanoparticles with monoclonal anti-fibronectin. (B) (i) 40 nm PSCOOH nanoparticles

binding to FNDC3A immobilised on protein microarrays at increasing human plasma concentrations and (ii) measurement of the fluorescence signal due to the bound particles. (C) Interaction network of FNDC3A according to the STRING algorithm showing interaction of fibronectin (FN1) with FNDC3A.

Protein corona evolution over a time course of incubation. For this analysis, PSCOOH nanoparticles were incubated in undiluted plasma (modeling *in vivo* conditions) for the following time series (10 minutes, 30 minutes, 1 hour and 4 hours) prior to incubation on the microarray. There are certain methodological limitations to the quantitative study of the corona kinetics using protein arrays, as array spot intensities are not fully quantitative, however they provide useful semi-quantitative information in regards to the nanoparticles interaction with the protein spotted on the array. DCS measurements (Figure 3a) confirmed nanoparticle protein corona stability as complexes are monodispersed and agglomeration was not detected over time. The nanoparticle/corona complex apparent diameter increased with time over two hours, where it reached a stationary plateau. Application of the sedimentation core shell model[3] to DCS data facilitated the estimation of the real protein shell thickness on nanoparticles surface where the apparent size of the nanoparticle protein corona complexes, compared to the pristine values, could be used to estimate the protein corona shell thickness knowing the density of the protein shell. Using this model the range of shell thickness was calculated to be approaching 1.5 nm. While the total protein amount remained constant, changes in intensities of particular gel bands were detected. For example, protein bands of 100kDa, 25kDa and 20kDa decreased with time, while the intensity of the 30kDa band increased with time, suggesting some degree of compositional rearrangement in the protein corona as a function of incubation time (Figure 3b). To correlate the protein corona time-evolution with the changes in the array interactome, nanoparticles have been pre-incubated with human plasma at the same time intervals and subsequently exposed to protein arrays. The total fluorescence intensity of nanoparticle positive hits (interactions between protein on the array and nanoparticle/corona complex) was monitored to evaluate the nanoparticles interactome profile (Figure S6a). Plotting the fluorescence intensities of the top 50 positive "hits" of each time-point on the array, revealed a similar number of high intensity interactions between nanoparticles and the arrayed proteins at different nanoparticles exposure times. While fluorescence intensities of top hits for 1, 3 and 4 hour array incubations have a similar trend, spot intensities of nanoparticles exposed to plasma for 10 minutes are significantly higher. This finding suggests that at 10 minutes of incubation, the protein corona is incompletely formed and higher intensity values might be caused by protein corona displacement by proteins spotted on the array. It is interesting to note that there was a correspondence between the decrease of fibronectin in the corona over time and an analogue reduction of the fluorescence intensity of the FNDC3A spot on the array (Figure S6b). While the strong decrease in the fluorescence intensity of the stronger protein binders between 10 min and 1 hour incubation in plasma was observed for all the spots, at longer times slight differences can be observed for the different proteins (Figure S7).

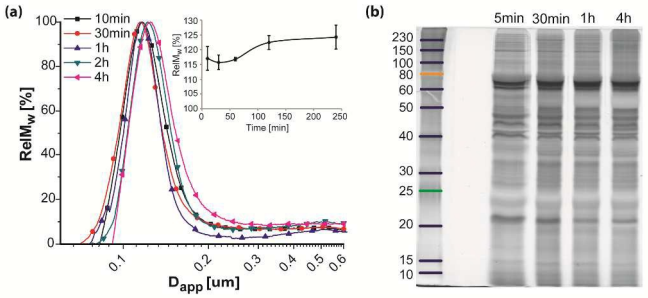

Time (min)	10	30	60	120	240
Apparent Diameter (nm)	117.0±4.0	115.8±2.5	116.8±0.6	122.5±2.3	124.3±4.0
Shell thickness (nm)	~9	~8.5	~8.8	~10	~10.3

Figure 3. a) The DCS results for evolution of PSCOOH nanoparticle corona complexes size with increasing nanoparticles exposition time to full human plasma. b) SDS-PAGE analysis of protein corona composition for nanoparticles exposed to human plasma for different times.

Discussion

In this study we have employed high content protein microarrays to gain an insight into how the protein corona on the surface of nanomaterials may interact with the biological environment through complexing with proteins expressed in that environment. From Figures 1a-b (40 nm PSCOOH nanoparticles) we see that for 10% (v/v) plasma concentration, the bare or pristine particle surface is relatively well covered and many of the main bound proteins are already defined, but the hard corona continues to evolve significantly to a concentration of 55% (v/v) plasma. In Figure 4, we show that whilst several arrayed proteins bind the pristine nanoparticle surface more strongly, the majority of the interactions (most of which are not shown) are similar to each other. This reflects the expectation that non-specific interactions between particle surface and typical proteins are similar across the array. The strength of all these bare surface-protein interactions decreases as the plasma concentration increases and most have reached their minimal level at 10% (v/v) plasma, presumably reflecting the typical energy scale of non-specific interactions between hard corona and target array proteins. In addition to plasma experiments, we have examined the binding profile in the context of a solution containing a single protein i.e., 10% (w/v) human serum albumin (HSA). In these experiments, a similar rapid decrease of the top 50 binding hits seen for each condition was seen and the majority of the interactions had a very low intensity. This overall behaviour is typical for all nanoparticles we have examined, though the details differ (data not shown). The key observation is that, amongst the thousands of array interactions that decrease as plasma concentration increases, several instead first decrease to a minimum (as described above), and then strongly increase with increasing plasma protein concentration (Table 2 and Figure S4). We interpret this to mean that the increased coverage of the nanoparticle surface lowers the general non-specific interaction with arrayed proteins, but that new specific biological recognition between corona proteins and arrayed proteins develops. Amongst these specific interactions, we identify here fibronectin domain containing 3A (FNDC3A), protein tyrosine phosphatase, non-receptor type 1 (PTPN1) and phosphatidylinositol binding clathrin assembly protein (PICALM).

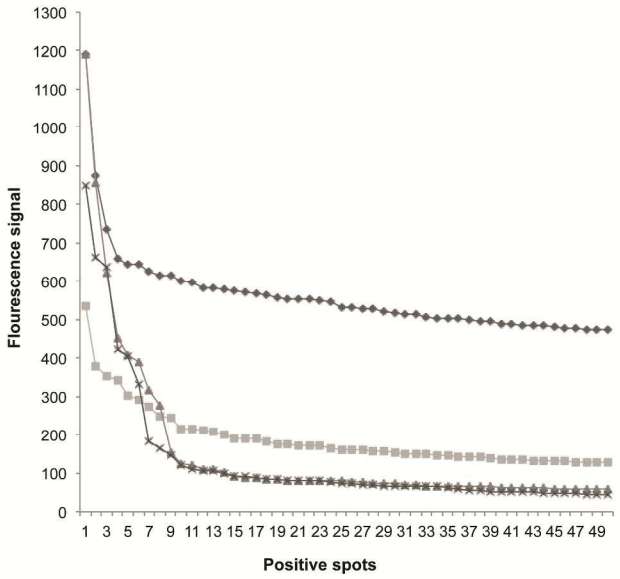

Figure 4. The ranked fluorescent intensities of the 50 highest positive spots incubated with 40 nm PSCOOH nanoparticles in increasing plasma concentration 0%(), 10%(), 55% () and 75%().

This characterization represents a further definition of the biological identity of the nanomaterial in the biological environment of plasma with implications for the behaviour for such materials *in vivo*. A particularly striking observation is made in the 40 nm hard corona, where the fibronectin content (derived from mass spectrometry and immunostaining, Figure 2 (i, ii)) grows significantly with increasing plasma, which then corresponds to a significant increase in binding to FNDC3A, a fibronectin binding receptor protein. Fibronectin Type III (FnIII) domains are one of the most common polypeptide topologies folds found in extracellular proteins. FnIII domains usually act as structural spacers, to arrange other domains in space as in fibronectin itself. However the FnIII domain can also play important functional roles by formation of protein-protein interfaces. normally expressed in the extracellular matrix.[31] In contrast, fibronectin is absent from the hard corona of 100nm nanoparticles (PSCOOH and $PSOSO_3$) at 10-55% plasma (Figure S2, Tables S6-S7) and there is no binding of these nanoparticle complexes to FNDC3A. FNDCA3 contains 9 fibronectin type III binding domains and has a functional interaction with fibronectin in cell adhesion and migration.[29] Such interactions may prove to be quite significant in the extrinsic interactions of nanomaterials in biological systems. There are other specific binding events, of course, for which there is no known origin in the catalogue of hard corona proteins, mitogen activated protein kinase 9 (MAPK9) and tyrosine protein phosphatase non-receptor type 1 (PTPN1) are two such examples (Table 2) where the initial signal decreases to very low values at 10% (v/v) plasma and then increases to a significantly higher signal than for the bare particle at elevated plasma concentration. This raises the intriguing possibility that entirely novel hard corona-target protein interactions can arise as a result of the specific nature of the hard corona packing and other details.

The study of protein corona evolution with time has shown that the corona formed after ten minutes incubation of nanoparticles in human plasma and it is not likely to be at equilibrium. The initial spread between repeats of shell thickness measurements and high total fluorescence intensity of 10 min array (Figure S8) can be attributed to corona formation dynamics at this early time point.

While it is natural to identify the origin of protein corona - protein interactions based on proteins identified in the averaged composition of the corona, there are several potential limitations to this approach. Firstly, commercially available protein arrays have a limited repertoire of proteins, and several of the hard corona proteins will not have suitable targets with which to bind on the array. Secondly, it is not evident that an abundant hard corona protein is present at a high density/concentration at the corona surface, and available for interaction. Third, corona protein-protein (and other) interactions could lead to novel interactions on the array, not easily predicted as a single corona protein-target array protein interaction. Finally, protein interaction databases (see for example the STRING algorithm; http://string-db.org/) are still incomplete, and many interactions are still not recorded.

We note how different the approach to use protein arrays incubated with nanoparticles is from the standard use of protein arrays in the study of protein interactions, essentially due to the context dependence of the interactions, and the overarching strong, non-specific, interactions of the bare particles with all arrayed proteins. We may also note that though the interactomes for different size PSCOOH nanoparticles are similar in buffer, they differ at the same surface area/protein ratio in human plasma, both in terms of composition and number of interactions above a given threshold (Figures S2-S3). We observe that 40 nm nanoparticles bind significantly higher numbers of microarray proteins at 10% (v/v) plasma than 100 nm nanoparticles with the same surface chemistry (Figures S8-S9), reflecting the fact that smaller particles (for fixed protein/total surface area ratios as in the present experimental conditions) present at a local level a higher surface curvature, which may influence the corona structure. This is reflected also in the DCS results (Figure 1), which show formation of a thinner protein shell for 40 nm nanoparticles in 10% (v/v) plasma than that of 100 nm PSCOOH nanoparticles (Figure S1), while comparable shell thickness and higher is reached at higher plasma concentrations. Still, the fact that the fully formed 'biological identity' of the nanoparticles may only emerge at higher plasma concentrations alerts us to potential differences in results from cell level and *in vivo* studies.[24, 32, 33] Moreover, for the same bulk material and the same size (100 nm PSCOOH and $PSOSO_3$ nanoparticles), the surface chemistry has a major impact on the extrinsic behaviour of the corona (Figure 5) due to the influence of the surface functional groups on the intrinsic (composition, structure, etc.) properties.

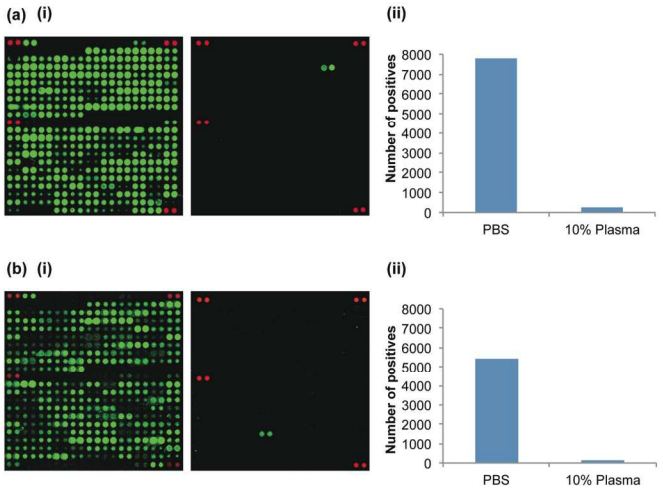

Figure 5. 100 nm polystyrene nanoparticles with distinct surface chemistry binding to human protein microarray. (A) 40 μg/ml PSCOOH nanoparticles in (i) PBS and (ii) 10% (v/v) human plasma with (iii) total numbers of positives in each condition. (B) 40 μg/ml $PSOSO_3$ nanoparticles in (i) PBS and (ii) 10% (v/v) plasma with (iii) total numbers of positives in each condition.

Conclusions

From a broader perspective, we have shown that imperfect surface coverage leads to non-specific interactions with numerous protein targets. However, for sufficiently complete nanoparticle surface coverage, the interactions between nanoparticle and the surrounding biological milieu leads to a remarkable new emergent biological identity, expressed by a few well defined nanoparticle-corona-protein interactions that bears no simple relation to the original nanomaterial itself. Such simple relations as exist between the original nanomaterial surface and emergent biological interactions appear (in several examples) related to the composition of the hard corona, but one should be alerted to the potential for entirely new interactions. The interactions (and means to assess them) reported here are of importance with respect to future explorations of cellular uptake, biodistributions, potential toxicity and other issues of practical interest.

Materials and Methods

Nanoparticles. Fluorescent Polystyrene latex beads, both carboxyl-modified PSCOOH (100 nm, 40 nm) and sulphonated-modified $PSOSO_3$ (100 nm), were purchased from Invitrogen. All nanoparticles were characterized by measuring their size and z-potential in physiological buffer before use. Both nanoparticle stock solutions and nanoparticles incubated in plasma were diluted with 10mM phosphate buffer at pH 7.4.

Human plasma preparation. Blood was withdrawn from 10-15 different volunteers and collected into 10 ml K_2EDTA coated tubes (BD Bioscience). Plasma was prepared following the HUPO BBB SOP guidelines. Briefly, immediately after blood collection, each tube was inverted ten times to ensure mixing of blood with the EDTA, and subsequently centrifuged for ten minutes at 1300 g at 4 ºC. Equal volumes of plasma from each donor were collected into a secondary 50 ml falcon tube and then centrifuged at 2400 g for 15 minutes at 4 ºC. Supernatant was collected (leaving approximately 10% of the volume in the secondary tube) and it was then divided into 1 ml cryovials and stored at -80ºC until use. Following this procedure the plasma protein concentration is estimated to be ~80 g/L, using BCA quantification (Pierce), in agreement with the literature.[34, 35]
When plasma was used for experiments, it was allowed to thaw at room temperature and centrifuged for 3 min at 16.2 kRCF. Thawed plasma was never re-frozen or re-thawed. All data presented are obtained using plasma from one donation session. The blood donation procedure was approved by the Human Research Ethics committee at University College Dublin.

Protein Microarray Incubation with Polystrene Nanoparticles. The Protoarray microarray slide (Invitrogen) was blocked by incubation in 1% skim milk powder dissolved in PBS with 1 mM DTT, 0.1% Tween 20 and 50% glycerol pH 7.5 for one hour and then washed once in PBS pH 7.5. The 40 and 100 nm PSCOOH nanoparticles and the $PSOSO_3$ 100 nm nanoparticles loaded with an orange fluorophore (Alexa 532nm, Invitrogen) were diluted from stock concentration of 20 mg/ml to 40, 5 and 1 μg/ml concentrations in a volume of 175 μl in physiological buffer, or in buffer containing human plasma diluted to a final concentration of 10-75% (v/v) or in 10% (v/v) human serum albumin. The nanoparticles were incubated in human plasma or HSA for 1 hour (or various amounts of time in case of protein corona evolution experiments) at room temperature prior to application to the microarray surface. The nanoparticle complexes were pipette onto the microarray surface and a coverslip was placed over the incubation for 1 hour. The slides were static throughout the incubation. Before imaging the slide was washed once in PBS and rinsed in deionized water. The slides were dried with centrifugation at 250 x g for 3 minutes. Imaging was performed using a Genepix 4000B scanner (Axon Instruments) with excitation at 532 nm and 635 nm.

Analysis of Microarray. Microarray slides were scanned in a Genepix 4000B scanner (Axon Instruments). The PMT gain settings were maintained at 500 and 250 for the 635 nm and 532 nm lasers respectively. The focus position was 10 μm. The microarrays used were all from the same lot and the gal file specific to the lot of microarrays was downloaded from the Invitrogen webpage. The .gpr result files from the array scans were analysed with Prospector software (Invitrogen) using small molecule fluorescence (SMF) settings.

The Prospector software (Invitrogen) was employed to analyse the fluorescent data derived from each spot when analysed with the lot specific gal file for the individual microarrays. The .GAL files were analysed using the "small molecule profiling – fluorescent" mode and the positive hits were determined based on two criteria:

- Signal ratio of individual protein features relative to the background on the array, calculated on a per-subarray basis, expressed as "Z-factor" >0.4 and
- Coefficient of variation for the signals from the two replicates less than 0.5

Mass spectrometry of nanoparticle protein corona. 100 and 40nm PSCOOH and 100nm $PSOSO_3$ nanoparticles were incubated in 10% human plasma to produce a specific protein corona as has been previously described.[23] These nanoparticles were then heat denatured at 95°C for 5 minutes in beta-mercaptoethanol containing Laemelli sample buffer and electrophoresed onto 10% polyacrylamide gels. The gel lanes were excised and the bands taken from each lane prior to trypsin digestion and mass spectrometry. All samples were run on

a Thermo Scientific LTQ ORBITRAP XL mass spectrometer connected to an Exigent NANO LC.1DPLUS chromatography system incorporating an auto-sampler. Tryptic peptides were resuspended in 0.1% formic acid. Each sample was loaded onto a Biobasic C18 PicofritTM column (100mm length, 75µm ID) and was separated by an increasing acetonitrile gradient, using a 120min reverse phase gradient (0-40% acetonitrile for 90 min) at a flow rate of 30nL min-1. The mass spectrometer was operated in positive ion mode with a capillary temperature of 200°C, a capillary voltage of 46V, a tube lens voltage of 140V and with a potential of 1800V applied to the frit. All data was acquired with the mass spectrometer operating in automatic data dependent switching mode. A high resolution MS scan was performed using the Orbitrap to select the 5 most intense ions prior to MS/MS analysis using the Ion trap. The raw mass spectral data was analyzed using Bioworks Browser 3.3.1 SP1, a proteomics analysis platform. All MS/MS spectra were sequence database searched using the algorithim TurboSEQUEST. The MS/MS spectra were searched against an IPI 3.5 database. The following search parameters were used: precursor-ion mass tolerance of 2 Da, fragment ion tolerance of 1.0 Da with methionine oxidation and cysteine carboxyamidomethylation specified as differential modifications and a maximum of 2 missed cleavage sites allowed.

Acknowledgements

This work was supported by the European Union's Seventh Framework Programme (EU FP7) under grant agreement no: 309329 (NANOSOLUTIONS), SFI PI Award (12/IA/1422; awarded to K.D.), SFI IP Award (12/IP/1620; awarded to D.O'C) the INSPIRE programme, funded by the Irish Government's Programme for Research in Third Level Institutions, Cycle 4, National Development Plan 2007-2013. The assistance of Kieran Wynne and Giuliano Elia of UCD Conway Mass Spectrometry Resource is gratefully acknowledged.

Author Contributions. D.O'C. and F.B.B. contributed equally to this manuscript. D.O'C, F.B.B., D.J.C, A.P, M.M, D.J.C and K.A.D. conceived and designed the experiments; D.O'C, F.B.B, M.M, A.P performed the experiments; D.O'C, F.B.B, A.P, M.M, D.J.C and K.A.D. analyzed the data. D.O'C, F.B.B, M.M and K.A.D. wrote the manuscript. All authors discussed the results and commented on the manuscript.

References

1. A. Salvati, A. S. Pitek, M. P. Monopoli, K. Prapainop, F. B. Bombelli, D. R. Hristov, P. M. Kelly, C. Aberg, E. Mahon and K. A. Dawson. Transferrin-functionalized nanoparticles lose their targeting capabilities when a biomolecule corona adsorbs on the surface *Nature nanotechnology*, 2013, **8**, 137-143.
2. I. Lynch, A. Salvati and K. A. Dawson. Protein-nanoparticle interactions: What does the cell see *Nature nanotechnology*, 2009, **4**, 546-547.
3. T. Cedervall, I. Lynch, S. Lindman, H. Nilsson, E. Thulin, S. Linse and K. A. Dawson. Understanding the nanoparticle protein corona using methods to quantify exchange rates and affinities of proteins for nanoparticles. *PNAS*, 2007, **104**, 2050-2055.
4. D. Walczyk, Baldelli Bombelli F., M. P. Monopoli, I. Lynch and K. Dawson. What the cell "sees" in Bionanoscience *JACS*, 2010, **132**, 5761-5768.
5. S. Wan, P. M. Kelly, E. Mahon, H. Stockmann, P. M. Rudd, F. Caruso, K. A. Dawson, Y. Yan and M. P. Monopoli. The "sweet" side of the protein corona: effects of glycosylation on nanoparticle-cell interactions *ACS nano*, 2015, **9**, 2157-2166.
6. A. E. Nel, L. Mädler, D. Velegol, T. Xia, E. M. V. Hoek, P. Somasundaran, F. Klaessig, V. Castranova and M. Thompson. Understanding biophysicochemical interactions at the nano–bio interface *Nature Materials*, 2009, **8**, 543-557.
7. X. Xin-Rui, N. A. Monteiro-Riviere and J. E. Riviere. An index for characterization of nanomaterials in biological systems *Nature nanotechnology*, 2010, **5**, 671-676.
8. E. Casals, T. Pfaller, A. Duschl, G. J. Oostingh and V. Puntes. Time Evolution of the Nanoparticle Protein Corona *ACS nano*, 2010, **4**, 3623-3632.
9. E. Hellstrand, Lynch I., A. Andersson, T. Drakenberg, B. Dahlback, K. Dawson, S. Linse and T. Cedervall. Complete high-density lipoproteins in nanoparticle corona *FEBS Journal*, 2009, **276**, 3372-3381.
10. M. A. Dobrovolskaia, A. K. Patri, J. W. Zheng, J. D. Clogston, N. Ayub, P. Aggarwal, B. W. Neun, J. B. Hall and S. E. McNeil. Interaction of colloidal gold nanoparticles with human blood: effects on particle size and analysis of plasma protein binding profiles *Nanomedicine-Nanotechnology Biology and Medicine*, 2009, **5**, 106-117.
11. S. Tenzer, D. Docter, J. Kuharev, A. Musyanovych, V. Fetz, R. Hecht, F. Schlenk, D. Fischer, K. Kiouptsi, C. Reinhardt, K. Landfester, H. Schild, M. Maskos, S. K. Knauer and R. H. Stauber. Rapid formation of plasma protein corona critically affects nanoparticle pathophysiology *Nature nanotechnology*, 2013, **8**, 772-781.
12. C. D. Walkey and W. C. Chan. Understanding and controlling the interaction of nanomaterials with proteins in a physiological environment *Chemical Society reviews*, 2012, **41**, 2780-2799.
13. B. Pelaz, G. Charron, C. Pfeiffer, Y. Zhao, J. M. de la Fuente, X. J. Liang, W. J. Parak and P. Del Pino. Interfacing engineered nanoparticles with biological systems: anticipating adverse nano-bio interactions *Small*, 2013, **9**, 1573-1584.
14. Z. J. Deng, L. Mingtao, M. Monteiro, I. Toth and R. F. Minchin. Nanoparticle-induced unfolding of fibrinogen promotes Mac-1 receptor activation and inflammation *Nature nanotechnology*, 2011, **6**, 39-44.
15. M. P. Monopoli, D. Walczyk, A. Campbell, G. Elia, I. Lynch, F. B. Bombelli and K. A. Dawson. Physical-chemical aspects of protein corona: relevance to in vitro and in vivo biological impacts of nanoparticles *Journal of the American Chemical Society*, 2011, **133**, 2525-2534.
16. C. Röcker, M. Pötzl, F. Zhang, W. J. Parak and G. U. Nienhaus. A quantitative fluorescence study of protein monolayer formation on colloidal nanoparticles *Nature nanotechnology*, 2009, **4**, 577-580.
17. P. Rivera Gil, G. Oberdorster, A. Elder, V. Puntes and W. J. Parak. Correlating physico-chemical with toxicological properties of nanoparticles: the present and the future *ACS nano*, 2010, **4**, 5527-5531.
18. G. W. Doorley and C. K. Payne. Cellular binding of nanoparticles in the presence of serum proteins *Chemical Communications*, 2011, **47**, 466-468.
19. S. Milani, F. B. Bombelli, A. S. Pitek, K. A. Dawson and J. Radler. Reversible versus irreversible binding of transferrin to polystyrene nanoparticles: soft and hard corona *ACS nano*, 2012, **6**, 2532-2541.
20. F. Bertoli, G. L. Davies, M. P. Monopoli, M. Moloney, Y. K. Gun'ko, A. Salvati and K. A. Dawson. Magnetic nanoparticles to recover cellular organelles and study the time resolved nanoparticle-cell interactome throughout uptake *Small*, 2014, **10**, 3307-3315.
21. A. S. Pitek, D. O'Connell, E. Mahon, M. P. Monopoli, F. Baldelli Bombelli and K. A. Dawson. Transferrin coated nanoparticles: study of the bionano interface in human plasma *PloS one*, 2012, **7**, e40685.
22. P. M. Kelly, C. Aberg, E. Polo, A. O'Connell, J. Cookman, J. Fallon, Z. Krpetic and K. A. Dawson. Mapping protein binding sites on the biomolecular corona of nanoparticles *Nature nanotechnology*, 2015, **10**, 472-479.
23. E. Casals, T. Pfaller, A. Duschl, G. J. Oostingh and V. F. Puntes. Hardening of the nanoparticle-protein corona in metal (Au, Ag) and oxide (Fe3O4, CoO, and CeO2) nanoparticles *Small*, 2011, **7**, 3479-3486.

24. G. Maiorano, S. Sabella, B. Sorce, V. Brunetti, M. A. Malvindi, R. Cingolani and P. P. Pompa. Effects of Cell Culture Media on the Dynamic Formation of Protein-Nanoparticle Complexes and Influence on the Cellular Response *ACS nano*, 2010, **4**, 7481-7491.
25. M. P. Monopoli, A. S. Pitek, I. Lynch and K. A. Dawson. Formation and characterization of the nanoparticle-protein corona *Methods in molecular biology*, 2013, **1025**, 137-155.
26. S. Linse , C. Cabaleiro-Lago, W. F. Xue, I. Lynch, S. Lindman, E. Thulin, S. E. Radford and K. A. Dawson. Nucleation of protein fibrillation by nanoparticles *PNAS*, 2007, **104**, 8691-8696.
27. A. M. W. Reed and S. J. Metallo. Oriented Protein Adsorption to Gold Nanoparticles through a Genetically Encodable Binding Motif *Langmuir : the ACS journal of surfaces and colloids*, 2010, **26**, 18945-18950.
28. D. Maiolo, P. Bergese, E. Mahon, K. A. Dawson and M. P. Monopoli. Surfactant titration of nanoparticle-protein corona *Analytical chemistry*, 2014, **86**, 12055-12063.
29. K. L. Obholz, A. Akopyan, K. G. Waymire and G. R. MacGregor. FNDC3A is required for adhesion between spermatids and Sertoli cells *Developmental Biology*, 2006, **298**, 498-513.
30. S. W. Shan, D. Y. Lee, Z. Q. Deng, T. Shatseva, Z. Jeyapalan, W. W. Du, Y. Zhang, J. W. Xuan, S. P. Yee, V. Siragam and B. B. Yang. MicroRNA MiR-17 retards tissue growth and represses fibronectin expression *Nature Cell Biology*, 2009, **11**, 1031-U1278.
31. I. D. Campbell and C. Spitzfaden. Building proteins with fibronectin type III modules *Structure*, 1994, **2**, 333-337.
32. C. Grabinski, N. Schaeublin, A. Wijaya, H. D'Couto, S. H. Baxamusa, K. Hamad-Schifferli and S. M. Hussain. Effect of Gold Nanorod Surface Chemistry on Cellular Response *ACS nano*, 2011, **5**, 2870-2879.
33. A. Lesniak, A. Campbell, M. P. Monopoli, I. Lynch, A. Salvati and K. A. Dawson. Serum heat inactivation affects protein corona composition and nanoparticle uptake *Biomaterials*, 2010, **31**, 9511-9518.
34. G. L. Hortin, D. Sviridov and N. L. Anderson. High-Abundance Polypeptides of the Human Plasma Proteome Comprising the Top 4 Logs of Polypeptide Abundance *Clinical Chemistry*, 2008, **54**, 1608-1616.
35. N. L. Anderson and N. G. Anderson. The human plasma proteome: history, character, and diagnostic prospects *Molecular & Cellular Proteomics*, 2002, **1**, 845-867.

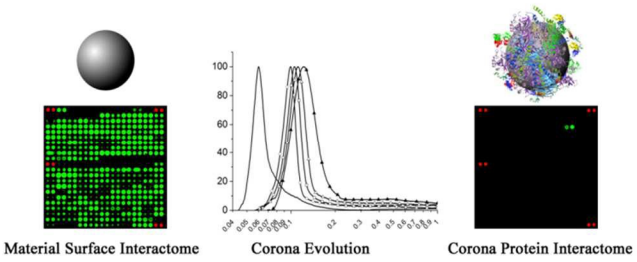

Nanoparticle biomolecular corona leads the interactions with cognate proteins on arrays of thousands of immobilised human proteins